Painting Crack Elimination Using Viscous Morphological Reconstruction

Allan Hanbury, Paul Kammerer and Ernestine Zolda*
Pattern Recognition and Image Processing Group
Vienna University of Technology
Favoritenstraße 9/1832, A-1040 Vienna, Austria
{Hanbury, Paul, Zolda}@prip.tuwien.ac.at

Abstract

A method for the elimination of cracks in infrared reflectograms is presented. Infrared reflectograms show the underdrawing – the basic concept of the artist drawn on the ground layer – in ancient wood panel paintings. Caused by different mechanical behaviour of the panel and the covering ground layer during the aging of the painting, cracks appear. Cracks not only disturb the appearance of a painting, but are also a problem for segmenting the lines and strokes of the underdrawing. A method based on mathematical morphology, namely morphological reconstruction with viscosity, is used to eliminate the cracks while keeping as much detail as possible in the brush strokes. A priori information that the cracks are usually thinner than the brush strokes and have a preferred orientation is taken into account.

1. Introduction

Computer aided analysis can be an important tool for the examination of works of art. An interdisciplinary project[1] between the fields of art history and image analysis is developing a system to investigate infrared images (infrared reflectograms [2]) of medieval and Renaissance panel paintings with methods of digital image processing and analysis.

The infrared reflectography technique allows the penetration of the covering paint layers and the visualisation of the underdrawing, the basic concept of a painter. The image depicted in Figure 1 gives an example of an underdrawing taken from a panel painting by an Austrian medieval painter. The sleeve region, covered by red pigments, could be penetrated by a CCD-camera in the spectral range between 700nm – 900nm. It shows the formation of strokes that sketch the crinkles in the top layer of the painting.

During the aging of the paintings, climactic fluctuations cause changes in the dimensionality of the panels. While younger pigment layers are elastic enough to follow contractions, a network of fine cracks (craquelé) may cover the whole painting during the aging process. The pattern of the cracks is determined by the background used. In the case of wooden panels, the cracks are primarily oriented perpendicular to the grain [6]. Willingen et al. [3] have studied the appearance of cracks and determined features to classify different types of cracks. They differentiate between features of individual cracks (smooth, jagged, depth, thickness etc.) and features of crack patterns (distance between cracks, type of junctions).

One major goal of the project is to identify the drawing tools used by the painter to create the underdrawing from the appearance of the strokes in the infrared reflectogram. A step toward the identification is the segmentation of the individual strokes. From the segmentation point of view, cracks are treated as structural noise and will produce artefacts in the segmentation step. To overcome this problem, our intention is to eliminate the cracks while keeping the boundaries of the strokes as accurately as possible for further analysis.

A similar problem has been treated by Giakoumis and Pitas [4]. They use a three step process which first detects the cracks using a top-hat operator, separates them from brush strokes using colour information, and then fills them in. In contrast to this work, we are working on greyscale images (recorded in the infra-red region). We therefore have no colour information for separating the cracks from the brush strokes. The information we start with is that the cracks are usually thinner than the brush strokes, and that they have a favoured orientation. To take this information into account, we make use of a morphological opening with a viscous reconstruction step, which detects the cracks and fills them in in one step. Abas and Martinez [1], on the other hand, are interested in the structure of the crack network. They use a top-hat operator to extract the cracks, and then extract descriptive information about the crack network so

*This work was supported by the Austrian Science Foundation (FWF) under grants P15471-MAT, P14445-MAT and P14662-INF.

[1] http://www.prip.tuwien.ac.at/Research/Casandra/index.html

Proceedings of the 12th International Conference on Image Analysis and Processing (ICIAP'03)
0-7695-1948-2/03 $17.00 © 2003 **IEEE**

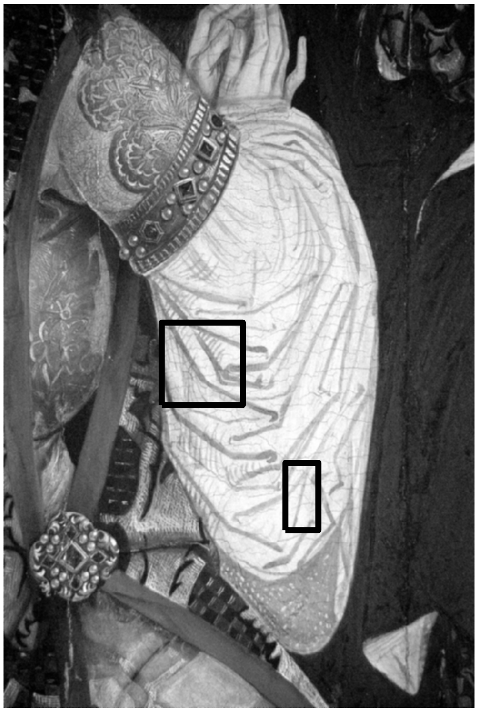

Figure 1. Infra-red image of medieval painting taken in the near IR-range. The black rectangles show the subregions used in figures 4 and 5.

as to classify it.

In section 2, we present the theory behind the viscous morphological reconstruction operator. The results of this operator applied to removing cracks from infra-red images of paintings are given in section 3.

2. Viscous Morphological Reconstruction

Viscous morphological reconstruction was introduced by Serra [7], who formulates it in a mathematically rigorous way in terms of viscous lattices. In this section, we give a brief application-oriented introduction to viscous reconstruction, beginning with an overview of standard morphological reconstruction [8].

With standard morphological reconstruction, one reconstructs a mask image from a marker image by iterating geodesic dilations of the marker image inside the mask image until stability. We denote by f the marker image and by g the mask image. Both these images have the same size, and $f \leq g$. The *geodesic dilation* with structuring element B_d of the marker image f with respect to the mask image g is

$$\delta_{B_d}^{(1)}(f, g) = \delta_{B_d}^{(1)}(f) \wedge g \tag{1}$$

where $\delta_{B_d}^{(1)}(f)$ indicates a dilation of image f by the structuring element B_d. The *reconstruction by dilation* of mask g from marker f, defined as the iteration of the geodesic dilation of marker f with respect to mask g until stability, is denoted

$$R_{B_d}(f, g) = \delta_{B_d}^{(i)}(f, g) \tag{2}$$

where i is chosen such that $\delta_{B_d}^{(i)}(f, g) = \delta_{B_d}^{(i+1)}(f, g)$. In general, the structuring element B_d is chosen to be the unit structuring element.

Viscous morphological reconstruction was introduced to solve a problem similar to the one shown in Figure 2. Figure 2a shows an area marked out by black circles on a white foreground. We wish to expand the marker shown in Figure 2b so that it fills out the region surrounded by the black circles. Obviously, a standard morphological reconstruction using Figure 2a as the mask and Figure 2b as the marker would produce Figure 2a as the result. The notion of viscosity was therefore introduced into the reconstruction process.

In order to incorporate viscosity, one performs an opening on the marker image after each geodesic dilation step. The *viscous geodesic dilation* of marker f with respect to mask g is defined as

$$\Delta_{B_d, B_o}^{(1)}(f, g) = \gamma_{B_o}\left[\delta_{B_d}^{(1)}(f, g)\right] \tag{3}$$

where B_d is, as before, the structuring element used for the geodesic dilation, and B_o is the structuring element used for the opening. As in equation 2, *viscous reconstruction by dilation* is defined as

$$R_{B_d, B_o}^{v}(f, g) = \Delta_{B_d, B_o}^{(i)}(f, g) \tag{4}$$

where i is chosen such that $\Delta_{B_d, B_o}^{(i)}(f, g) = \Delta_{B_d, B_o}^{(i+1)}(f, g)$.

As a demonstration of viscous reconstruction, we reconstruct the marker in Figure 2b inside the mask in Figure 2a, using a disc of radius r for both structuring elements B_d and B_o. For values of $r < 24$ pixels, one obtains the initial mask (Figure 2a) as a result, as the spacing between at least one pair of points is wider than 48 pixels. When $r = 24$ pixels, the result shown in Figure 2c is obtained. Here, the reconstruction has been constrained to lie inside the surrounding points. This corresponds to the largest reconstructed region constrained by the points. If the radius is further increased (i.e. $r > 24$ pixels), then the reconstruction cannot penetrate into the narrower parts between the points, as is seen in Figure 2d, which shows a reconstruction for a disc with $r = 32$ pixels. Serra [7] demonstrates a method for obtaining a line which approximates the distribution of the points. One calculates the maximum reconstruction within

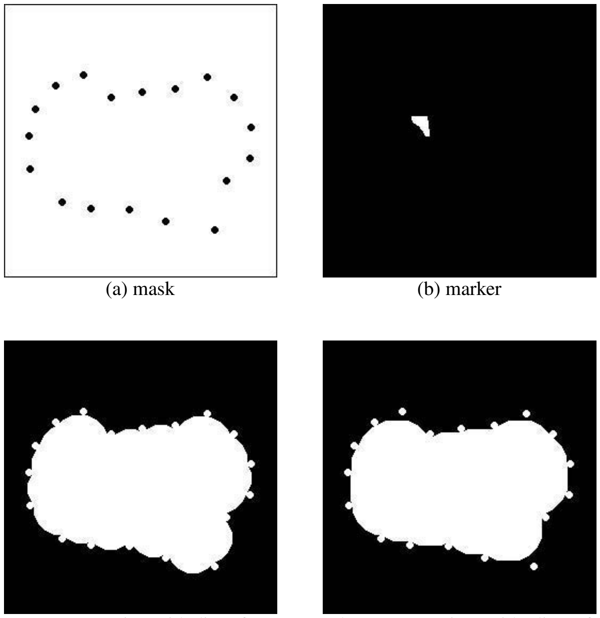

(a) mask (b) marker

(c) reconstruction with disc of radius 24 pixels (d) reconstruction with disc of radius 32 pixels

Figure 2. Viscous morphological reconstruction of the mask (a) from the marker (b) using: (c) a disc of radius 24 pixels and (d) a disc of radius 32 pixels for both structuring elements B_d and B_o. Images are of size 256 by 256 pixels.

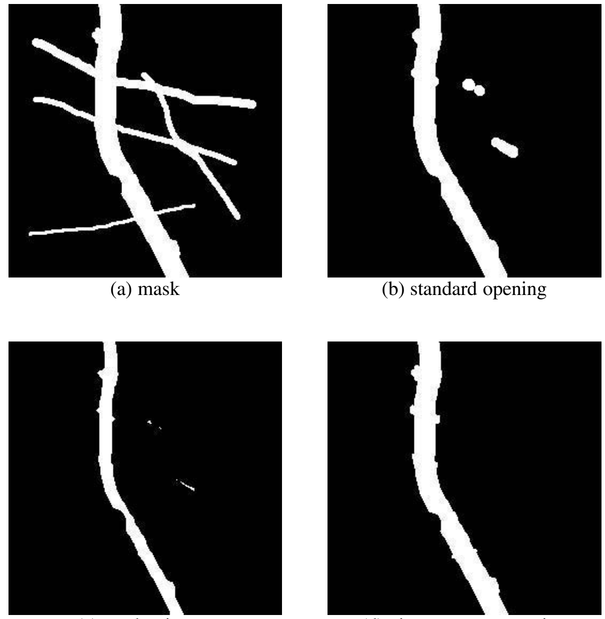

(a) mask (b) standard opening

(c) marker image (d) viscous reconstruction

Figure 3. (a) Initial image. (b) Opening of image (a) with a disc of radius 5 pixels. (c) Marker image obtained by eroding image (a) with a disc of radius 5 pixels. (d) Viscous reconstruction for mask (a) from marker (c). Images are of size 256 by 256 pixels.

the points (as done above) and the maximum reconstruction starting from a marker lying outside the points. The median line of the intersection of these two reconstructions gives a good representation of the outline of the area sketched out by the points.

In the context of this paper, we are interested in the ability of the viscous reconstruction to reconstruct small details while preventing certain elements from being reconstructed. The challenges faced in the art history application are illustrated schematically in the simple binary example shown in Figure 3a. In this image, we wish to preserve the thick line and all its details as accurately as possible, while removing the thin lines which intersect it. The thin lines are known to have a diameter of less than 10 pixels, but intersections can sometimes result in thicker regions. An opening of Figure 3a with a disc-shaped structuring element of radius 5 is shown in Figure 3b. As expected, the details on the thick line have been smoothed, however, not all the thin lines have been successfully removed. Using a larger structuring element would smooth the thick line even more, and reconstruction cannot be used as the thin lines intersect the thick line, and would therefore be reconstructed too.

The use of viscous reconstruction is a good solution to this problem. We begin by creating the marker image shown in Figure 3c by eroding Figure 3a by a disc of radius 5 pixels. To reconstruct the initial image, we use equation 4, with B_d a 3×3 pixel square, and B_o a disc of radius 5 pixels. In order to reconstruct the small details, we append an extra geodesic dilation onto the reconstruction algorithm. The result of this reconstruction is shown in Figure 3d.

It remains to discuss some practical details of the use of viscous reconstruction. The first is the choice of the structuring elements B_d and B_o. If one wants to ensure that all regions in the marker image are used as seeds for the reconstruction process, then B_d should be the same size as B_o, as in the first example discussed. Alternatively, if B_d is set to the unit structuring element (or any structuring element smaller than B_o), then any regions in the marker image which are smaller than B_o after the first geodesic dilation with B_d will be eliminated. This is potentially useful, as it allows less severe filters to be used in the creation of the marker image. This is demonstrated in the example of

Figure 3, where even though not all the thin lines are eliminated in the creation of the marker, they still do not appear in the result. The second implementation detail to discuss is the addition of an extra geodesic dilation at the end of the reconstruction procedure. For the first example, this is not recommended as one aims to keep the reconstructed area inside the markers, and the extra geodesic dilation step will certainly expand it further into the exterior region. For the second example, where we wish to preserve small details on the thick line being reconstructed, this additional geodesic dilation is useful.

Having demonstrated the use of viscous reconstruction operators on binary images, we now move onto their application to the removal of thin cracks in greyscale images.

3. Application to the removal of cracks

We present a comparison between various mathematical morphology based methods of removing cracks from infra-red images of paintings. For this example, we use Figure 4a, which corresponds to the lower sub-region indicated in Figure 1. Note that all morphological operations in this section are performed on the inverse of Figure 4a so that the objects to be removed are lighter than the background, as this simplifies the use of the reconstruction operator. The resulting images shown have been inverted again.

An obvious way of removing the cracks which are smaller than a given size is to use a morphological opening with a disc which has a diameter larger than the cracks, but smaller than the brush strokes. The result of such an opening with a disc of radius 6 is shown in Figure 4b. This approach has the disadvantage of leaving a number of artefacts corresponding to the shape of the structuring element, and of smoothing the boundaries of the strokes. The standard way of keeping the strokes as similar to the original as possible is to reconstruct the original image (mask) from an image eroded by the same disc used before (marker), which is shown in Figure 4c. In this case, however, the cracks are reconstructed too, as they have a similar greylevel and are connected to the brush strokes.

In order to avoid reconstructing the narrow cracks, reconstruction with viscosity can be used, with the structuring element used to do the opening (B_o in equation 4) set to a disc slightly larger than the cracks. Figure 4d shows the result of this viscous reconstruction, which uses an erosion of the (inverted) initial image by a disc of radius 6 pixels as the marker. It is clear that this image contains fewer background artefacts than the image resulting from a standard opening (Figure 4b). For the viscous reconstruction, structuring element B_d is set to a 3×3 square, and B_o to a disc-shaped structuring element of the same size as for the initial erosion (6 pixels). The main reason for the disappearance of the cracks which were still visible after the standard opening (Figure 4b) is the additional opening performed during the reconstruction process. After one unit dilation, the cracks remaining in the marker image get eliminated by this opening, as they are not wide enough to survive.

Due to this extra ability of the reconstruction process to remove cracks, it is not necessary to use such a large structuring element during the initial erosion. We therefore decided to take some extra a priori information into account during this erosion, namely that a large majority of the cracks have a preferred orientation, as discussed in the introduction. For the image under consideration, this preferred orientation is horizontal. We therefore take as our marker image an erosion of the initial image by a vertical line of length 10 pixels, shown in Figure 4e. The viscous reconstruction from this marker image, using a 3×3 pixel square for B_d, and a disc-shaped structuring element of radius 6 for B_o, is shown in Figure 4f. It is clear that while the cracks are eliminated as efficiently as before, more structure remains in the strokes.

Potential problems with this method arise when brush strokes are of a similar thickness to the cracks. In contrast to the work in [4], we do not have any colour information allowing us to distinguish between the two. Further information, such as the smoothness of the lines, will potentially have to be taken into account in difficult cases. An example of such a difficult case is shown in Figure 5a, the upper sub-region indicated in Figure 1. The same parameters were used to calculate the viscous reconstruction shown in Figure 5b as for the previous example, that is, the marker was created by eroding the initial image with a vertical line of length 10 pixels, and the viscous reconstruction was done with a 3×3 pixel square for B_d, and a disc of radius 6 for B_o. In the reconstruction, many of the light, thin brush strokes in the complicated left half of the image are also eliminated.

4. Conclusion

We have demonstrated the application of viscous morphological reconstruction to an art history problem dealing with the analysis of infra-red reflectograms of ancient panel paintings. In these reflectograms, it is required that the thin lines (the cracks) be eliminated, while retaining as much detail as possible in the thicker lines (the brush strokes). The greylevels of the cracks and the brush strokes are similar, and the fact that they intersect prohibits the use of standard morphological reconstruction. Other available a priori information which has been taken into account is that the cracks have a preferred orientation due to the mechanical properties of the wood on which the painting was done. The suggested approach functions well except in more complicated regions of a painting where the brush strokes have a similar width to the cracks. Further work on separating

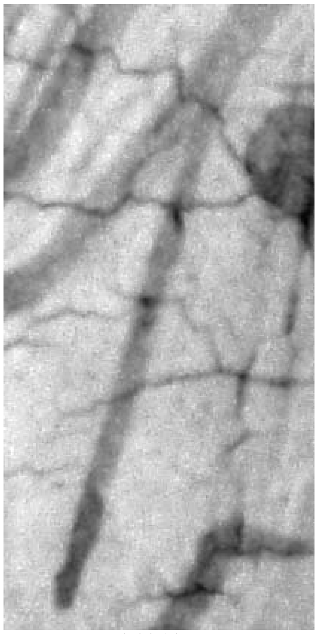

(a) initial image

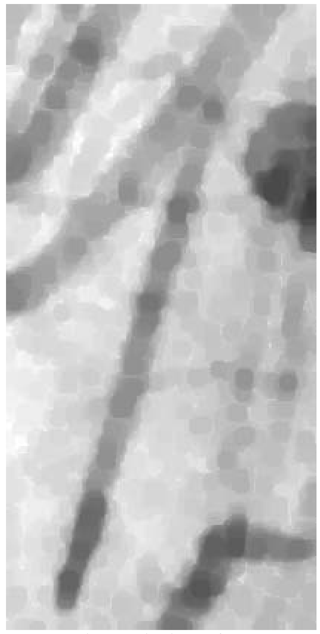

(b) standard opening

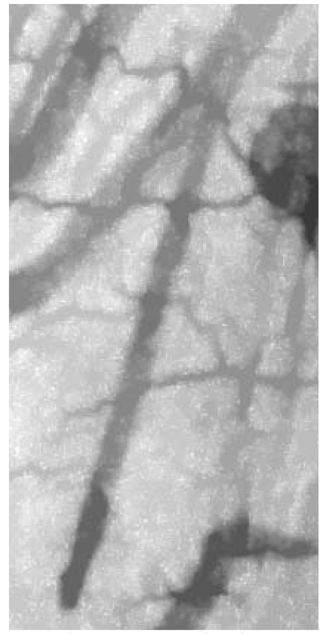

(c) ordinary reconstruction from erosion by disc SE

(d) viscous reconstruction from erosion by disc SE

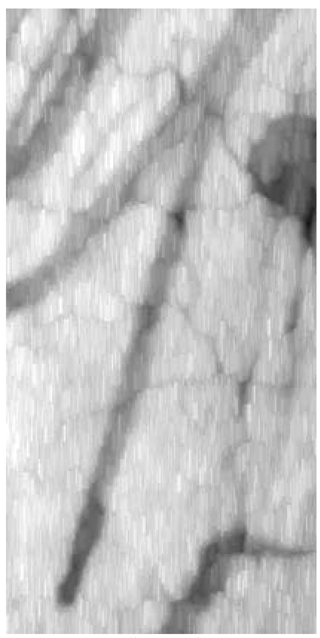

(e) line erosion

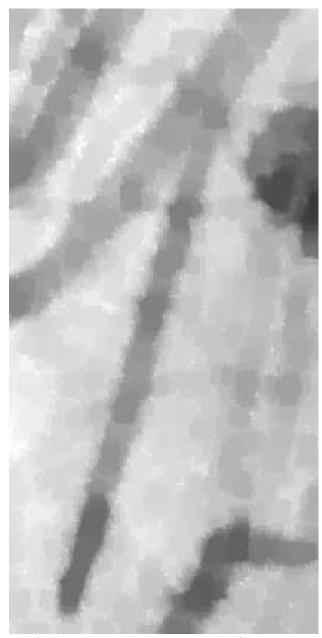

(f) viscous reconstruction from (e)

Figure 4. (a) Initial image. (b) Standard opening of (a) with a disc of radius 6 pixels. (c) Reconstruction of (a) using as marker an erosion of (a) by a disc of radius 6 pixels. (d) Viscous reconstruction of (a) from the marker used for image (c). (e) Erosion of (a) by a vertical line of length 10 pixels. (f) Viscous reconstruction of (a) using (e) as a marker.

(a) initial image

(b) viscous reconstruction

Figure 5. (a) A difficult image from which to remove cracks. (b) A reconstruction with viscosity of image (a).

strokes and cracks based on their smoothness remains to be done.

Further applications of viscous morphological reconstruction exist. It has been used, for example, in determining a poorly-visible outline of a heart muscle in a positron image [7]. In the context in which it has been applied here, it could be interesting to apply it to scratch removal in motion picture restoration. Such scratches have a similar orientation specificity to the cracks on paintings, being always vertically oriented with respect to the images [5].

Acknowledgements

Thank you to Thomas Walter of the Centre de Morphologie Mathématique, Ecole des Mines de Paris, France, for help in the implementation of the viscous reconstruction operator.

References

[1] F. S. Abas and K. Martinez. Classification of painting cracks for content-based analysis. In *Proceedings of IS&T/SPIE's 15th Annual Symposium on Electronic Imaging: Machine Vision Applications in Industrial Inspection XI*, 2003.

[2] J. V. A. de Boer. *Infrared Reflectography. - A Contribution to the Examination of Earlier European Paintings*. PhD thesis, Univ. Amsterdam, 1970.

[3] P. de Willigen. A mathematical study on craquelure and other mechanical damage in paintings. Technical report, Delft University of Technology, Faculty of Information Technology and Systems, Department of Mathematics and Computer Science, 1999.

[4] I. Giakoumis and I. Pitas. Digital restoration of painting cracks. In *Proceedings of the IEEE Int. Symposium on Circuits and Systems (ISCAS '98)*, 1998.

[5] L. Joyeux, O. Buisson, B. Besserer, and S. Boukir. Detection and removal of line scratches in motion picture films. In *Proceeding of the IEEE Conference on Computer Vision and Pattern Recognition*, volume 1, pages 548–553, 1999.

[6] F. Mairinger. *Strahlenuntersuchung an Kunstwerken*. E. A. Seemann, Berlin, 2003.

[7] J. Serra. Les treillis visqueux. Technical Report N-51/99/MM, CMM, Ecole des Mines de Paris, 1999.

[8] P. Soille. *Morphological Image Analysis: Principles and Applications*. Springer-Verlag, 1999.